EPJ Web of Conferences **175**, 13017 (2018) https://doi.org/10.1051/epjconf/201817513017
Lattice 2017

The K_L - K_S Mass Difference

Ziyuan Bai[1], *Norman H.* Christ[1], and *Christopher T.* Sachrajda[2,⋆]

[1] *Physics Department, Columbia University, New York, NY 10027, USA*
[2] *Department of Physics and Astronomy, University of Southampton, Southampton SO17 1BJ, UK*

Abstract. We review the status of the RBC-UKQCD collaborations' computations of the K_L-K_S mass difference. After a brief discussion of the theoretical framework which had been developed previously by the collaboration, we describe our latest computation, performed at physical quark masses, and present our preliminary result $m_{K_L} - m_{K_S} = (5.5 \pm 1.70) \times 10^{-12}$ MeV.

1 Introduction

The value of the K_L-K_S mass difference, $\Delta m_K \equiv m_{K_L} - m_{K_S} = 3.483(6) \times 10^{-12}$ MeV, is truly tiny on the scale of $\Lambda_{\rm QCD}$. This *flavour-changing neutral current* (FCNC) process is therefore an excellent one in which to search for the effects of new physics. For example if we imagine an effective new-physics $\Delta S = 2$ contribution of the form $\frac{1}{\Lambda^2}(\bar{s}\cdots d)(\bar{s}\cdots d)$, where the ellipses represent possible Dirac matrices, and if we could reproduce the experimental Δm_K in the SM to 10% accuracy then we would be sensitive to scales $\Lambda \gtrsim (10^3 - 10^4)$ TeV. This illustrates the sensitivity of precision flavour physics to scales which are unreachable directly at the Large Hadron Collider.

The mass difference Δm_K is obtained from second order weak perturbation theory, specifically:

$$\Delta m_K \equiv m_{K_L} - m_{K_S} = 2\mathcal{P} \sum_\alpha \frac{\langle \bar{K}^0 \,|\, H_W \,|\, \alpha \rangle \langle \alpha \,|\, H_W \,|\, K^0 \rangle}{m_K - E_\alpha} = 3.483(6) \times 10^{-12}\,\text{MeV}\,, \tag{1}$$

where the sum over the intermediate states $|\alpha\rangle$ includes an integration over the relevant phase-space and H_W is the effective weak Hamiltonian density.

The calculation of Δm_K is one component of the RBC-UKQCD collaborations' programme of computations of long-distance contributions in kaon physics, requiring the evaluation of matrix elements of bilocal operators of the form

$$\int d^4x \, \langle f \,|\, T[Q_1(x)\, Q_2(0)] \,|\, i \rangle \,. \tag{2}$$

Other applications being studied include the rare-kaon decays $K \to \pi\ell^+\ell^-$ [1, 2] and $K^+ \to \pi^+\nu\bar{\nu}$ [3, 4] and the indirect CP-violation parameter ϵ_K [5]. Progress on all these topics is summarised by X. Feng at this conference [6]. As well as computing the non-perturbative long-distance contributions from scales of $O(\Lambda_{\rm QCD})$, we aim to avoid the necessity of performing perturbation theory at the scale of m_c. For Δm_K this has proved particularly slowly convergent [7].

⋆ Speaker, e-mail: cts@soton.ac.uk

1.1 Status of earlier RBC-UKQCD calculations of Δm_K

Before presenting our new results we briefly summarise our previous work. In [8] we developed the framework necessary for the calculation of Δm_K as well as performing an exploratory calculation on a $16^3 \times 32$ lattice with unphysical masses ($m_\pi = 421\,\text{MeV}$) and including only the connected diagrams. However, the results were encouragingly, and perhaps surprisingly, reasonably close to the experimental value. This was followed by a calculation of all the diagrams on a $24^3 \times 64$ lattice with inverse lattice spacing $a^{-1} = 1.729(28)\,\text{GeV}$ and with the unphysical masses $m_\pi = 330\,\text{MeV}$, $m_K = 575\,\text{MeV}$, $m_c^{\overline{\text{MS}}}(2\,\text{GeV}) = 949\,\text{MeV}$ [9]. For these parameters we found $\Delta m_K = 3.19(41)(96)\,\text{MeV}$.

In this talk we will present an update of the computations and preliminary results obtained at physical masses.

2 The theoretical framework

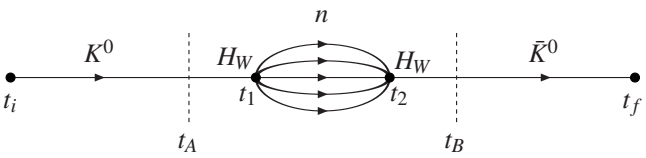

Figure 1. Representation of the four-point correlation function C_4 from which Δm_K is determined.

In this section we briefly review the theoretical framework used in the computation of Δm_K [8, 9]. In fig.1 we sketch the four-point correlation function used to determine Δm_K. The K^0 ($\bar{K}^0$) is created (annihilated) at t_i (t_f) and the two weak effective Hamiltonians are inserted at times $t_{1,2}$ which are integrated over the interval (t_A, t_B). With all the states at rest, the correlation function is given by

$$C_4(t_A, t_B; t_i, t_f) = |Z_K|^2 e^{-m_K(t_f - t_i)} \sum_n \frac{\langle \bar{K}^0 \,|\, H_W \,|\, n\rangle \langle n \,|\, H_W \,|\, K^0\rangle}{(m_K - E_n)^2} \left\{ e^{(m_K - E_n)T} - (m_K - E_n)T - 1 \right\}, \quad (3)$$

where $T = t_B - t_A + 1$, $Z_K = \langle K^0 \,|\, \phi_K^\dagger(0) \,|\, 0\rangle$ and $\phi_K^\dagger$ is the interpolating operator used to create the kaon. From the coefficient of T in eq.(3) we obtain

$$\Delta m_K^{\text{FV}} \equiv 2 \sum_n \frac{\langle \bar{K}^0 \,|\, H_W \,|\, n\rangle \langle n \,|\, H_W \,|\, K^0\rangle}{(m_K - E_n)}, \quad (4)$$

which should be compared to the infinite-volume expression in eq.(1). The superscript FV in Δm_K^{FV} stands for Finite Volume. The finite-volume corrections necessary to relate Δm_K^{FV} in (4) to Δm_K in (1) have been derived in [10].

The presence of terms in eq. (3) which grow exponentially with T when there are intermediate states $|n\rangle$ with energies E_n which are smaller than m_K is a generic feature of the calculation of matrix elements of bilocal operators. The freedom to add terms of the form $c_S\, \bar{s}d$ and $c_P\, \bar{s}\gamma^5 d$, where $c_{S,P}$ are constants, to H_W without changing Δm_K allows us to remove two such contributions. We choose c_P such that $\langle 0 \,|H_W + c_P \bar{s}\,\gamma^5 d|K^0\rangle = 0$. A natural choice for c_S would be such as to remove the single-pion intermediate state. However, although $m_\eta > m_K$, the contribution from the η is noisy and we find it numerically advantageous to eliminate this contribution. We therefore chose c_S such that $\langle \eta \,|H_W + c_S\, \bar{s}d|K^0\rangle = 0$. This leaves us the single-pion and two-pion states to evaluate using three-point functions and to remove the corresponding growing exponentials.

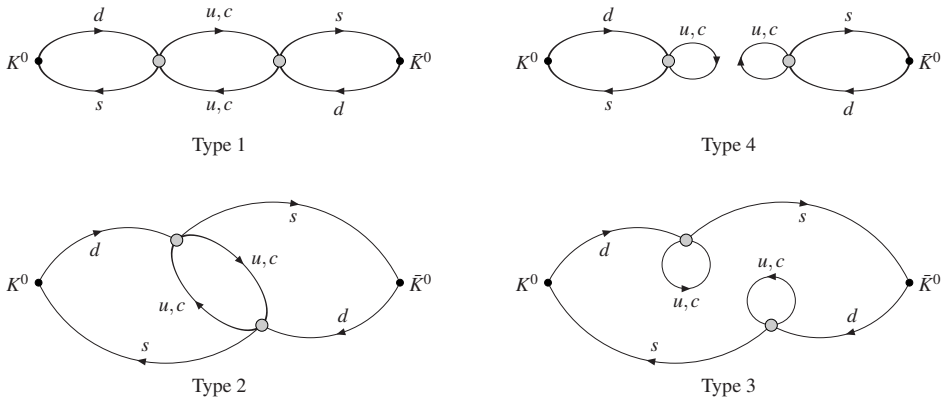

Figure 2. The four types of diagram contributing to the $K^0 \to \bar{K}^0$ transition. The shaded circles represent the insertion of the effective weak Hamiltonian.

2.1 Ultraviolet divergences in the calculation of Δm_K

The $\Delta S = 1$ effective Weak Hamiltonian takes the form:

$$H_W = \frac{G_F}{\sqrt{2}} \sum_{q,q'=u,c} V_{qd} V^*_{q's} (C_1 Q_1^{qq'} + C_2 Q_2^{qq'}) \tag{5}$$

where the $\{Q_i^{qq'}\}_{i=1,2}$ are current-current operators, defined as:

$$Q_1^{qq'} = (\bar{s}_i \gamma^\mu (1-\gamma^5) d_i)\,(\bar{q}_j \gamma^\mu (1-\gamma^5) q'_j) \quad \text{and} \quad Q_2^{qq'} = (\bar{s}_i \gamma^\mu (1-\gamma^5) d_j)\,(\bar{q}_j \gamma^\mu (1-\gamma^5) q'_i)\,. \tag{6}$$

As the separation between the two H_W operators decreases, we have the potential of new ultraviolet divergences. The diagrams contributing to the K^0-$\bar{K}^0$ transition correlation function are presented in fig.2. Consider for example the Type1 diagram. Power counting suggests that the contribution from the u-quark in the central loop would lead to a quadratic divergence. However, the $V-A$ nature of the currents together with the GIM mechanism leads to the elimination of both the quadratic and logarithmic divergences. Thus once the local operators $Q_{1,2}$ are renormalised, no new ultraviolet divergences arise. This is not the case for ϵ_K or for $K \to \pi\nu\bar{\nu}$ rare kaons decays, where additional divergences are present and need to be renormalised [3].

3 Details of the simulation

The calculation is being performed on a $L^3 \times T \times L_s = 64^3 \times 128 \times 12$ lattice, using Möbius Domain Wall Fermions and the Iwasaki gauge action; more details about the ensemble can be found in [11]. The inverse lattice spacing a^{-1}=2.359(7) GeV and the light and strange quark masses correspond to $m_\pi = 135.9(3)$ MeV and $m_K = 496.9(7)$ MeV (very close to the physical masses of the neutral pion $m_{\pi^0} = 134.98$ MeV and kaon $m_{K^0} = 497.6$ MeV). In studies of charm physics on these configurations, the bare mass of the charm quark was determined to lie in the range $am_c \simeq 0.32$ - 0.33. Our results presented below were obtained using $am_c = 0.31$, but we have also studied the dependence on m_c finding it to be mild when compared to the overall uncertainties (see tables 1 and 2 below).

The correlation functions which need to be evaluated are illustrated diagrammatically in fig.2. The shaded circles represent the insertion of the effective weak Hamiltonian given in eq.(5) so that

for each such diagram there are 4 contractions which need to evaluated, and we distinguish three types of quark propagators used in their evaluation.

1. We use Coulomb-gauge wall-source propagators for the d and s quarks at the K^0 source and $\bar{K}^0$ sink on each time slice. The d-quark propagators are obtained using standard low-mode deflation techniques. The lowest 2000 eigenvalues and the corresponding eigenvectors are obtained using the Lanczos algorithm. The full propagators are then obtained using the conjugate gradient algorithm, with a *sloppy* stopping residual of 10^{-4} on all configurations and an *exact* one of 10^{-8} on a small subset of configurations. These sloppy and exact propagators are used in the *all mode averaging* (AMA) [12] procedure, as described below. For the s-quark propagator we simply use the conjugate gradient algorithm.

2. For the connected diagrams, i.e.those of type 1 and 2, on each time slice we generate point-source propagators at a single spacial point which corresponds to the position of one of the weak operators in fig.2. The spacial position of the source is varied from time-slice to time-slice; specifically for time slice $0 < t < 127$, the source is placed at the point $(4t(\text{modulo } L), 4t(\text{modulo } L), 4t(\text{modulo } L))$. These propagators connect to the position of the second insertion of the weak Hamiltonian, which is summed over all space so that momentum is conserved.

The point-source propagators for the u quark are also determined using low-mode deflation as described above. However, as explained below, they are only used in measurements of type 1 and 2 diagrams with exact propagators and so are only computed for a small subset of configurations. The point-source c-quark propagators are determined using the conjugate-gradient algorithm.

3. For the u-quark self-loops in the diagrams of type 3 and 4 we use the 2000 low-mode eigenvectors and eigenvalues mentioned above and complete the construction of the all-to-all propagators stochastically using 60 random space-time volume sources for each configuration. For the c-quark in these loops, the propagators are obtained stochastically with the same random sources as for the u quarks.

The preliminary results presented below were obtained on a subset of 59 configurations for the noisier type-3 and type-4 diagrams, using AMA with *sloppy* propagators corrected by including measurements with exact propagators on a subset of 7 configurations. The less noisy type-1 and type-2 diagrams were calculated on 11 configurations with exact stopping conditions for the propagators. An indication of the computational cost is about 5 hours on a 8K BG/Q machine for each sloppy measurement and 15 hours for an exact one. The contributions from the different diagrams are combined and the uncertainties are determined using the superjacknife procedure [13]. In addition, for the disconnected type 4 diagrams, which are the most noisy, the left and right-hand sides, see Fig.2, are stored separately for the K^0 source and $\bar{K}^0$ sink in order to enable us to vary the source-sink separation. For the diagrams of type 1, 2 and 3 the positions of the K^0 source and $\bar{K}^0$ sink are varied over all values of t_i and t_f but their separation $t_f - t_i$ is fixed to be 48.

4 Preliminary Results

In the left-hand plot of fig.3 we show the integrated correlation functions as a function of T for each pair of operators (Q_i, Q_j) $(i, j = 1, 2)$. The mass difference Δm_K is obtained from the slope of the correlation function with T and in the figure we obtain the slopes by fitting the correlation function in the range $10 \leq T \leq 20$. From the slopes we obtain $\Delta m_K^{\text{FV}} = (5.8 \pm 1.7)\, 10^{-12}$ MeV. We now make a number of comments about this result.

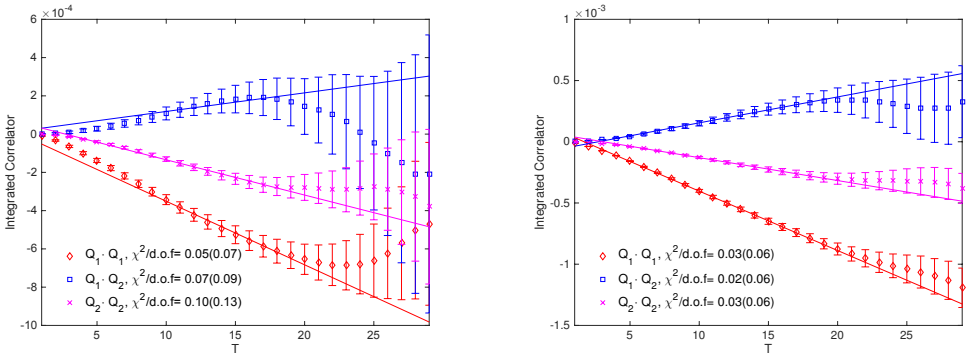

all diagrams Type 1 & 2 diagrams only

Figure 3. Left-hand plot: the correlation functions for pairs of operators (Q_i, Q_j) with all diagrams included. Right-hand plot: the same but neglecting type 3 and type 4 diagrams. The lines represented uncorrelated fits in the range $10 \leq T \leq 20$.

1. As the superscript in $\Delta m_K^{\rm FV}$ indicates, finite-volume corrections still need to be applied. A preliminary study of these, presented in section 4.3 below, suggests that they are small on the scale of our uncertainties but further work is needed to confirm this.

2. We find that at this stage we do not have sufficient statistics to obtain a reliable covariance matrix and hence to perform correlated fits. Recall that for the type 1 and 2 diagrams we currently have measurements on 11 configurations.

3. In the right-hand plots of figure 3 we present the contributions to the correlation functions from the type 1 and 2 diagrams; these give the larger contribution. Had we estimated $\Delta m_K^{\rm FV}$ using only these diagrams we would have found $\Delta m_K^{\rm FV\,1\&2} = (7.0 \pm 1.3)\, 10^{-12}$ MeV (the corresponding contribution from the type 3 and 4 diagrams is $\Delta m_K^{\rm FV\,3\&4} = -(1.1 \pm 1.2)\, 10^{-12}$ MeV).

In the remainder of this section we expand on three aspects of the calculation, the dependence of the results on the charm-quark mass, the renormalisation of $Q_{1,2}$ and the finite-volume corrections.

4.1 Dependence on the mass of the charm quark

In order to profit from the GIM cancellation of the additional ultraviolet divergences when the two operators in the diagrams of fig.2 approach each other we work in the four-flavour theory with a charm quark as indicated in the figure. From the collaborations' exploratory studies of charm-quark physics we anticipate that the physical bare charm quark mass for this ensemble is $am_c \simeq 0.32 - 0.33$[1]. The main results presented here have been obtained with $am_c = 0.31$, but we have also studied the dependence of the result on m_c on 56 configurations and the results are presented in table 1. Given the relatively large uncertainties in the results, in order to study whether the m_c dependence is significant we present in table 2 the jackknife differences $\Delta m_K(m_c) - \Delta m_K(0.25)$. We conclude that the dependence of Δm_K on the mass of the charm-quark appears to be mild on the scale of our current uncertainties. We also do not observe any sudden behaviour of the results with m_c up to $am_c = 0.34$ which would have signalled a breakdown due to large lattice artefacts.

[1] T.Tsang, private communication.

Table 1. The dependence of Δm_K on the mass of the charm quark.

am_c	0.25	0.28	**0.31**	0.34
ΔM_K	4.7(19)	5.1(18)	5.5(20)	5.9(21)

Table 2. The jackknife differences $\Delta m_K(m_c) - \Delta m_K(0.25)$.

am_c	0.28	0.31	0.34
ΔM_K	0.38(66)	0.78(65)	1.23(80)

4.2 Renormalisation of the effective weak Hamiltonian

Since there are no new ultraviolet divergences arising from the region of integration/summation where the separation of the two effective weak Hamiltonians approaches 0, the necessary renormalizsation is that of the two operators $Q_{1,2}$. Since $Q_1 \pm Q_2$ belong to different representations of SU(4) (20 and 84) they renormalize multiplicatively and we need to determine the corresponding two multiplicative renormalisation constants. In the $Q_{1,2}$ basis this results in a renormalisation matrix with $Z_{11} = Z_{22}$ and $Z_{12} = Z_{21}$ (see eq. (7) below). We proceed as is standard by first renormalising the two operators in a RI-SMOM scheme [14] and then matching this perturbatively to the $\overline{\rm MS}$ scheme (see sec.III of ref.[8] for the description of the procedure as applied to Δm_K, noting however that in the present study we use the (γ^μ, γ^μ) as the intermediate RI-SMOM scheme and not $(\gamma^\mu, \not{q})$ as used in [8]).

1. The non-perturbative renormalisation is performed on an ensemble [15] with smaller $32^3\times64$ lattice volume generated with the same bare coupling but with a heavier than physical light quark mass and with the Shamir rather than the Mobius DWF action. The difference in the light quark masses should lead to a negligible error associated with our substitution of this $32^3 \times 64$ ensemble because the NPR calculation is performed at large momenta. However, the difference between the Shamir and Mobius actions may lead to as much as 1% difference between the renormalisation factors computed on the $32^3\times64$ ensemble and those appropriate for the $64^3\times128$ ensemble being used to compute ΔM_K. (Here 1% was the difference in lattice spacings found between these two, nearly identical ensembles [11].)

The non-exceptional kinematics defining the (γ^μ, γ^μ) RI-SMOM scheme used here is defined by $d(p_1)\bar{s}(-p_2) \to s(p_2)\,\bar{d}(-p_1)$ [16] with $p_1 = (4,4,0,0)$ and $p_2 = (0,4,4,0)$ in lattice units so that $p_1^2 = p_2^2 \simeq 7\,\mathrm{GeV}^2$. The corresponding renormalisation matrix $Z^{\rm lat\to RI\text{-}SMOM}$ is found to be

$$\begin{pmatrix} Q_1^{\rm RI\text{-}SMOM} \\ Q_2^{\rm RI\text{-}SMOM} \end{pmatrix} = Z^{\rm lat\to RI\text{-}SMOM} \begin{pmatrix} Q_1^{\rm latt} \\ Q_2^{\rm latt} \end{pmatrix} = \begin{pmatrix} 0.6266 & -0.0437 \\ -0.0437 & 0.6266 \end{pmatrix} \begin{pmatrix} Q_1^{\rm latt} \\ Q_2^{\rm latt} \end{pmatrix}. \tag{7}$$

The errors on the entries in $Z^{\rm lat\to RI\text{-}SMOM}$ are negligible (typically 1 on the final figure) and the results were obtained from 3 configurations.

2. Writing the matching matrix from the RI-SMOM scheme to $\overline{\rm MS}$ in the form

$$Q_i^{\overline{\rm MS}} = (I + \Delta r)_{ij}\, Q_j^{\rm RI\text{-}SMOM} \tag{8}$$

an extension of [17] gives[2]

$$\Delta r = \begin{pmatrix} -2.2817\cdot10^{-3} & 6.8452\cdot10^{-3} \\ 6.8452\cdot10^{-3} & -2.2817\cdot10^{-3} \end{pmatrix}. \tag{9}$$

[2]C.Lehner, private communication.

3. Finally we use the perturbatively calculated Wilson coefficients in the $\overline{\text{MS}}$ scheme from [18], $C_1^{\overline{\text{MS}}}(7.0\,\text{GeV}^2) = -0.2600$ and $C_2^{\overline{\text{MS}}}(7.0\,\text{GeV}^2) = 1.1179$.

4.3 Finite-volume corrections

The non-exponential finite-volume effects come from the contribution of the two-pion states to the correlation function and are given by [10]

$$\Delta m_K^{FV} = 2\mathcal{P}\int \text{dE}\,\rho_V(E)\frac{f(E)}{m_K - E} - 2\sum_n \frac{f(E_n)}{m_K - E_n} = -2\left(f(m_K)\cot(h)\frac{dh}{dE}\right)_{E=m_K}, \tag{10}$$

where $\rho_V(E)$ is the (infinite-volume) density of states with an energy E; i.e. it is the factor relating $f(E)$ which is defined in the finite volume to the corresponding infinite-volume integrand. On the right-hand side of eq.(10)

$$f(m_K) = {}_V\langle \bar{K}^0|H_W|(\pi\pi)_{E=m_K}\rangle_V\ {}_V\langle(\pi\pi)_{E=m_K}|H_W|K_0\rangle_V \quad \text{and} \quad h(k) = \delta(k) + \phi(k)\,. \tag{11}$$

In eq. (11) δ is the s-wave two-pion phase-shift (the $I = 0$ channel is the dominant one) and ϕ is the kinematic function defined by Lüscher [19] (the quantisation condition for two-pions in the s-wave and a particular isospin state is $\tan(\phi + \delta) = 0$). See ref. [10] for further details.

The phase-shift $\delta(k_{m_K})$ and its derivative are unknown from this calculation and so we can only estimate the finite-volume correction. Provisionally, we do this very approximately by determining the $\pi\pi$ scattering length $a_{\pi\pi}$ and using the linear approximation $\delta(k_{m_K}) = k_{m_K}\, a_{\pi\pi}$. With this approximation the finite-volume correction is found to be much smaller than the total statistical uncertainty, $\Delta m_K^{\text{FV}} = -0.27(18) \times 10^{-12}$ MeV. Further studies, using other theoretical or model estimates of $\delta(k_{m_K})$ and its derivative are needed to improve this estimate and to reduce its uncertainty. However, given the small contribution of the two-pion states to Δm_K we anticipate that the correction will remain small. We find that the contribution of the $I = 0$ two-pion state to Δm_K is $(-0.027 \pm 0.015) \times 10^{-12}$ MeV.

5 Summary and Conclusions

We have performed the first non-perturbative calculations of $\Delta m_K \equiv m_{K_L} - m_{K_S}$, now with physical quark masses. In this talk have presented our preliminary result:

$$\Delta m_K = (5.5 \pm 1.7) \times 10^{-12}\,\text{MeV}\,. \tag{12}$$

(The physical value is $(\Delta m_K)^{\text{phys}} = 3.483(6)\times 10^{-12}$ MeV .) The result in eq. (12) includes the estimate of the finite-volume corrections discussed above and the quoted error is statistical only.

Our immediate plan is to complete the current calculation by performing measurements on 160 configurations with the aim of reducing the statistical uncertainty to about 1.0×10^{-12} MeV. The systematic uncertainties need to be studied further; these include assigning an error due to the uncertainty in m_c and the corresponding discretisation effects, as well as a more detailed study of the finite-volume corrections. In addition, the result in (12) does not include any uncertainty in the Wilson coefficient functions, both in the original calculations in the $\overline{\text{MS}}$ scheme and in the matching between the non-perturbative RI-SMOM scheme to $\overline{\text{MS}}$. While these are obtained in perturbation theory, so that higher order calculations will reduce any uncertainty, lattice calculations can also help by using step-scaling to increase the energy scale at which the matching is performed. Ultimately one might hope that lattice computations can be used to determine the Wilson coefficient functions without the need for perturbative calculations (see e.g. [20] presented at this conference).

In the longer term and on the next generation of machines we will develop a strategy to include an improved determination of Δm_K together with other elements of the RBC-UKQCD kaon physics programme (see e.g. X.Feng's talk at this conference[6]). The precise determination of Δm_K in the standard model and the comparison to the physical value $(\Delta m_K)^{\rm phys} = 3.483(6) \times 10^{-12}\,\text{MeV}$ is an important example of the use of the use of flavour physics to search for inconsistencies and to constrain models of new physics.

Acknowledgements We warmly thank our colleagues from the RBC-UKQCD collaborations for creating the scientific environment which enabled this project to be possible and to flourish. Z.B. and N.H.C. were supported in part by DOE Grant de-sc0011941 and CTS was supported in part by STFC Grant ST/L000296/1. An award of computer time was provided by the INCITE program. This research used resources of the Argonne Leadership Computing Facility, which is a DOE Office of Science User Facility supported under Contract DE-AC02-06CH11357.

References

[1] N.H. Christ, X. Feng, A. Portelli, C.T. Sachrajda (RBC, UKQCD), Phys. Rev. **D92**, 094512 (2015), 1507.03094
[2] N.H. Christ, X. Feng, A. Juttner, A. Lawson, A. Portelli, C.T. Sachrajda, Phys. Rev. **D94**, 114516 (2016), 1608.07585
[3] N.H. Christ, X. Feng, A. Portelli, C.T. Sachrajda (RBC, UKQCD), Phys. Rev. **D93**, 114517 (2016), 1605.04442
[4] Z. Bai, N.H. Christ, X. Feng, A. Lawson, A. Portelli, C.T. Sachrajda, Phys. Rev. Lett. **118**, 252001 (2017), 1701.02858
[5] Z. Bai, PoS **LATTICE2016**, 309 (2017), 1611.06601
[6] X. Feng, *Recent Progress in applying lattice QCD to kaon physics*, in *Proceedings, 35th International Symposium on Lattice Field Theory (Lattice2017): Granada, Spain* (2018)
[7] J. Brod, M. Gorbahn, Phys. Rev. Lett. **108**, 121801 (2012), 1108.2036
[8] N.H. Christ, T. Izubuchi, C.T. Sachrajda, A. Soni, J. Yu (RBC, UKQCD), Phys. Rev. **D88**, 014508 (2013), 1212.5931
[9] Z. Bai, N.H. Christ, T. Izubuchi, C.T. Sachrajda, A. Soni, J. Yu, Phys. Rev. Lett. **113**, 112003 (2014), 1406.0916
[10] N.H. Christ, X. Feng, G. Martinelli, C.T. Sachrajda, Phys. Rev. **D91**, 114510 (2015), 1504.01170
[11] T. Blum et al. (RBC, UKQCD), Phys. Rev. **D93**, 074505 (2016), 1411.7017
[12] T. Blum, T. Izubuchi, E. Shintani, Phys. Rev. **D88**, 094503 (2013), 1208.4349
[13] J.D. Bratt et al. (LHPC), Phys. Rev. **D82**, 094502 (2010), 1001.3620
[14] C. Sturm, Y. Aoki, N.H. Christ, T. Izubuchi, C.T.C. Sachrajda, A. Soni, Phys. Rev. **D80**, 014501 (2009), 0901.2599
[15] Y. Aoki et al. (RBC, UKQCD), Phys. Rev. **D83**, 074508 (2011), 1011.0892
[16] Y. Aoki et al., Phys. Rev. **D84**, 014503 (2011), 1012.4178
[17] C. Lehner, C. Sturm, Phys. Rev. **D84**, 014001 (2011), 1104.4948
[18] G. Buchalla, A.J. Buras, M.E. Lautenbacher, Rev. Mod. Phys. **68**, 1125 (1996), hep-ph/9512380
[19] M. Luscher, Nucl. Phys. **B354**, 531 (1991)
[20] M. Bruno, *Weak Hamiltonian Wilson coefficients from lattice QCD*, in *Proceedings, 35th International Symposium on Lattice Field Theory (Lattice2017): Granada, Spain* (2018)